Surface-Grafting of Ground Rubber Tire by Poly Acrylic acid via Self-Initiated Free Radical Polymerization and Composites with Epoxy Thereof

Sriram Yagneswaran,[1] William J. Storer,[1] Neetu Tomar,[2] Manuel N. Chaur,[2] Luis Echegoyen,[2] Dennis W. Smith Jr[1]

[1]*Department of Chemistry and The Alan G. MacDiarmid Nanotech Institute, The University of Texas at Dallas, Richardson, Texas 75080*

[2]*Department of Chemistry, School of Material Science and Engineering and Center for Optical Materials Science and Engineering Technologies (COMSET), Clemson University, Clemson, South Carolina 29634*

Commercially available recycled ground rubber tire (GRT) particles, found to contain persistent mechano-free radicals confirmed by electron paramagnetic spectroscopy for the first time self-initiates free radical polymerization of acrylic acid (AA). The poly acrylic acid (PAA) grafted GRT (PAA-*g*-GRT) was confirmed by Attenuated Total Reflection Fourier Transform Infrared spectroscopy, X-ray photoelectron spectroscopy, and thermogravimetric analysis (TGA). Epoxy composites using the PAA-*g*-GRT as filler were prepared and their mechanical properties were studied. The PAA-*g*-GRT/epoxy composite showed higher mechanical properties with an increase of modulus up to 180% as compared with the neat GRT/epoxy composite. Surface morphology of GRT, neat GRT/epoxy, and PAA-*g*-GRT/epoxy composites were analyzed by scanning electron microscopy. This technology introduces a new concept to functional and reactive recycling and the cost effective utilization of renewable resource green materials. POLYM. COMPOS., 34:769–777, 2013. © 2013 Society of Plastics Engineers

INTRODUCTION

Rubber represents the second largest used commodity after oil, in particular to its consumption in the automotive industry [1]. After use, these tires are discarded primarily in a landfill thereby creating a threat to the environment and economy [2]. Millions of scrap tires are stockpiled each year around the world. In an effort toward solving these problems, several approaches have been done to recycle the scrap tire. However, such methods have proved to be uneconomical and inefficient [3]. Utilization of ground rubber tires (GRT) as filler is an important step toward an effective and inexpensive recycling approach [4]. GRT particles are produced by grinding under two different processing conditions, ambient grinding, and cryogenic grinding. The demerits of the ambient processes [5] have led to a new type of cryogenically aided mechanochemical turbo-shearing mill grinding process for producing engineered GRT particles of controlled particle size and distribution [6].

Various researchers have reported the application of GRT particles as filler in rubber-modified asphalt, thermoplastics, and thermosetting polymer matrices. Applicability of polymeric fillers for a particular end-use application is largely depended on the surface chemistry. Therefore, the chemical modification of these rubber particles becomes necessary [7, 8]. Surface modification of GRT using different methods such as plasma treatment, corona discharge, halogenation, high energy radiation, UV, ion and photoinduced grafting, and using chemical initiator have been reported [9, 10].

Previously, modification of GRT particles by pretreatment with sulfuric acid to improve the compatibility between GRT particles and high density polyethylene matrix was attempted [11]. Further chemical modifications of the GRT particles have been done using nitric acid, hydrogen peroxide, and halogen [12]. Improvement in the properties of surface-chlorinated GRT/polyvinyl chloride blend was reported by Naskar et al. [13, 14]. The effect of UV induced grafting of bis-maleimide on the mechanical performance of the GRT/natural rubber blends and UV-initiated photografting of different vinyl monomers

Correspondence to: Dennis W. Smith; e-mail: dwsmith@utdallas.edu
Manuel N. Chaur is currently at Universidad del Valle, Cali, Colombia.
Luis Echegoyen is currently at Department of Chemistry, The University of Texas at El Paso, Texas 79968, USA.
Contract grant sponsor: The University of Texas at Dallas and Robert Welch Foundation; contract grant number: AT-0041.
DOI 10.1002/pc.22484
Published online in Wiley Online Library (wileyonlinelibrary.com).

onto low-density polyethylene matrix in the presence of initiator have also been reported [12].

Pittolo and Burford [15] synthesized semi-interpenetrating networks by swelling peroxide cross-linked polybutadiene and styrene butadiene rubber powders in styrene monomer and subsequent homopolymerization. Photoinitiated grafting of GRT by glycidyl methacrylate and methacrylic acid was carried out by Fuhrmann and Karger-Kocsis [16]. Coiai et al. grafted polymers on GRT by atom transfer radical polymerization and free-radical radical polymerization [17, 18]. Recently, our group in collaboration with Michelin Corporation reported a hydrosilylation method for surface modification of the GRT particles with and without solvents and catalysts (Karsted's/Pt Catalyst) followed by hydrolysis to obtain silanol functionalized GRT [19, 20]. More recently, Aggour et al. [21] reported the surface modification of waste tire by styrene and maleic anhydride.

In this work, we demonstrate the first self-initiated surface-grafting of cryogenically grinded mechanochemically devulcanized GRT particles by poly acrylic acid (PAA) via free radical polymerization. The stable free radicals (mechano-free radicals) present in the GRT initiate the polymerization. The obtained PAA-*g*-GRT is used as fillers in the formation of composites with epoxy resin. The free radicals found in the as-received GRT are confirmed by electron paramagnetic spectroscopy (EPR). The synthesized PAA-*g*-GRT and PAA-*g*-GRT/epoxy composites are characterized by Attenuated Total Reflection Fourier Transform Infrared (ATR-FTIR), X-ray photoelectron spectroscopy (XPS), thermogravimetric analysis (TGA), and scanning electron microscopy (SEM). In addition, mechanical properties are studied.

EXPERIMENTAL

Materials

Acrylic acid (AA, 99.5% pure) was purchased from Acros Organics, USA. Diglycidylether of bisphenol A epoxy (Floropoxy 4805 part A, equivalent weight = 188) and polyoxyalkyleneamine (U0-161 part B, equivalent weight = 60), the activator for the epoxy system, were purchased from FLOROCK, USA. Cryogenically grinded mechanochemically devulcanized GRT (PolyDyne, 80 Mesh size) was generously donated by Lehigh Technologies (Atlanta, GA). All the materials were used as received.

Synthesis of PAA-g-GRT

In a 100 ml round bottom flask, 30 ml of AA, and 5 g of GRT were mixed and purged with nitrogen gas for 15 min. The flask was heated at 80–85°C for 1 h with a stirring speed of 350 rpm. The reaction was carried out at different time intervals (1, 3, 6, and 12 h). The obtained product was soxhlet-extracted in water for 24 h to remove any residual monomer and ungrafted polymer. It was found that 4–5 times of washing with boiling water is equivalent to the soxhlet extraction. Thus, this procedure was used for subsequent experiments. The percentage of grafting was calculated by the following equation.

$$\text{Graft}\% = \frac{\text{W} - \text{W0}}{\text{W0}} \times 100$$

where W_0 and W are the weight of GRT before and after surface-grafting of PAA. The grafting percentage increases from 4 to 10% as the reaction time increases from 1 to 12 h. The as-synthesized PAA-*g*-GRT at a given time interval of 12 h with a grafting yield of 10% was chosen in our study.

Epoxy Resin Cross-Linking

The epoxy curing or cross-linking process was carried out by mechanically stirring the epoxy resin and polyoxyalkyleneamine activator (stoichiometric ratio, amine: epoxy, 1:3) at 60°C for 1 h. The mixture was then placed into a preheated mold and degassed under vacuum for 30 min. The obtained samples were cured at 50°C for 90 min, and then postcured at 120°C for a period of 24 h.

Synthesis of PAA-g-GRT/Epoxy Composites

PAA-*g*-GRT/epoxy composites were prepared by mechanically stirring the epoxy resin and different weight fraction of PAA-*g*-GRT (5, 10, 20, 30, and 40 wt% with respect to epoxy resin) at 60°C for 1 h. After cooling, polyoxyalkyleneamine activator (amine:epoxy, 1:3) was added and stirred homogeneously. The mixture was then placed into a preheated mold and degassed under vacuum for 30 min. The obtained samples were cured at 50°C for 90 min, and then postcured at 120°C for a period of 24 h. Similarly, the neat GRT/epoxy composites were also prepared.

Characterization

EPR spectrum of cryo-ground GRT particles was measured using a Bruker EMX spectrometer. Equal amount of each sample was placed in a 3 mm O.D. quartz tube and the experiments were performed at room temperature. ATR-FTIR spectrum was recorded using a Shimadzu spectrometer from 4000 to 600 cm^{-1} wavenumber range. Thermal analysis (TGA/SDTA 851, Mettler Instruments Toledo) was carried out at a heating rate of 10°C min^{-1} under nitrogen from ambient temperature to 800°C. The mechanical properties were tested under ambient condition at a crosshead speed of 2 mm min^{-1} using the universal testing machine (Instron Model 5969) with 50 kN capacity. Dumbbell-shaped specimens were made according to ASTM-638-99 standards for tensile

 DOI 10.1002/pc

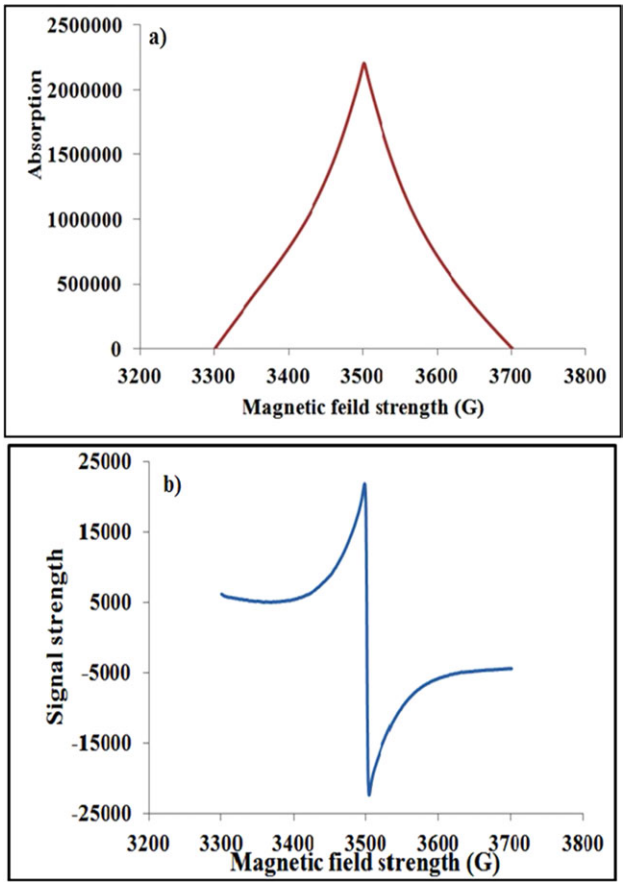

FIG. 1. EPR spectrum of GRT (a) absorption spectrum and (b) first derivative spectrum. [Color figure can be viewed in the online issue, which is available at wileyonlinelibrary.com.]

strength and modulus measurements, while flexural properties were determined by a three-point bending method in accordance with ASTM D-790 standard. At least five samples for each composite composition were tested.

RESULTS AND DISCUSSION

The as-received GRT is a complex mixture of different additives, such as oils, curatives, antioxidants, and other

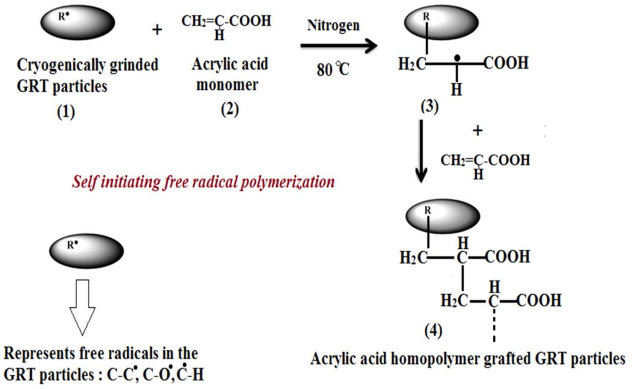

Scheme 1. Proposed mechanism for the self-initiated grafting of AA on the GRT surface. [Color figure can be viewed in the online issue, which is available at wileyonlinelibrary.com.]

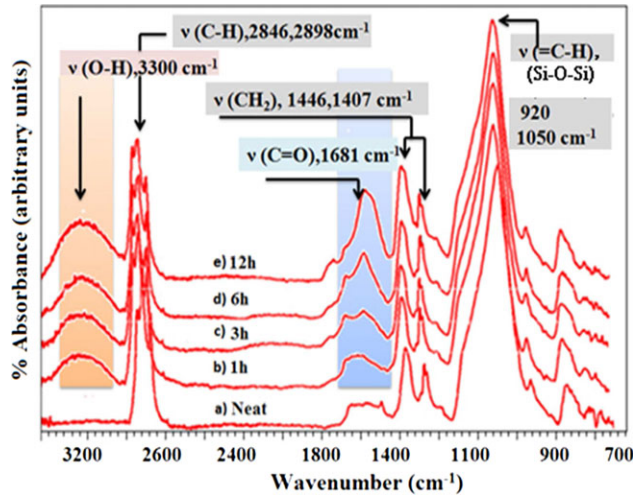

FIG. 2. ATR-FTIR spectra of the (a) neat GRT and (b-e) PAA-*g*-GRT at different time intervals. [Color figure can be viewed in the online issue, which is available at wileyonlinelibrary.com.]

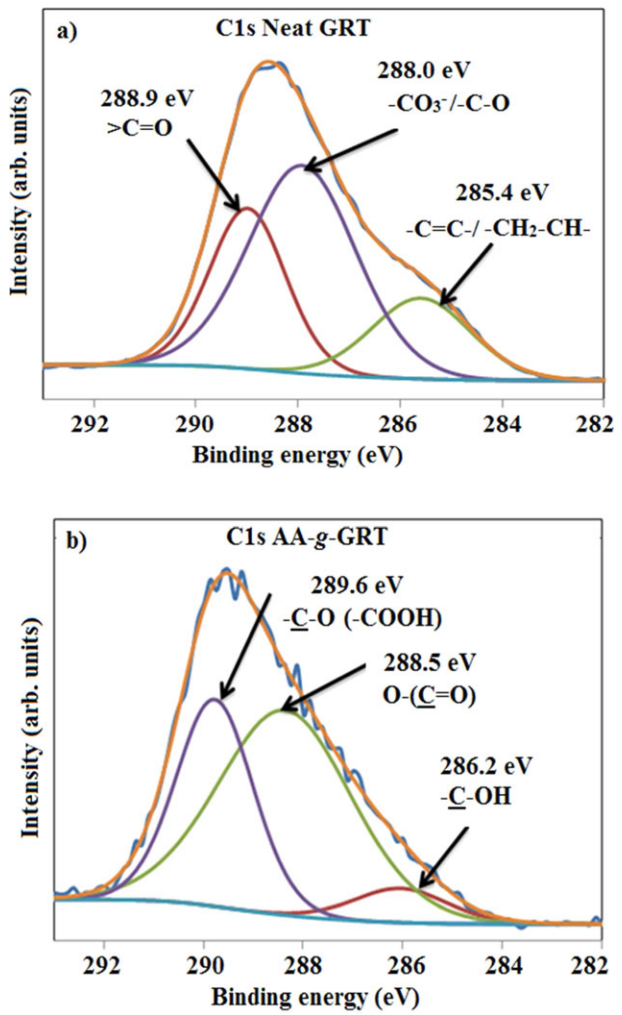

FIG. 3. C1s core level XPS spectra of the (a) neat GRT and (b) PAA-*g*-GRT. [Color figure can be viewed in the online issue, which is available at wileyonlinelibrary.com.]

materials added during the tire manufacturing processes. The principle components present in the as-received GRT are reprocessed rubber (NR-SBR; 40–45%), carbon black (27–33%), zinc oxide (0.2–0.3%), silica (0.2–0.3%), sulfur (1.5–2.5%), zinc stearate (1–2%), and process oil (10–20%) according to the supplier's statement.

EPR Analysis

EPR is a powerful technique for the quantitative analysis of the presence of free radicals. The as-received GRT particles found to contain persistent mechano-free radicals is supported by EPR analysis. Like most spectroscopic techniques, EPR spectrometer measures the absorption of electromagnetic radiation. However, a phase-sensitive detector is used in EPR spectrometer, which converts the normal absorption signal to its first derivative. Figure 1 shows the absorption and first derivative spectrum of GRT. The intensity of the signal is proportional to the concentration of free-radical species. The first derivative spectrum showed (Fig. 1b) a relatively broader feature with a sharp superimposed singlet with a g-factor of 2.0035, which is in close agreement with the free electron g-factor of 2.0023. This value is indicative of carbon or hydrocarbon-based free radicals. The g-factor was calculated according to the following equation.

$$g = \frac{hv}{\mu BH}$$

where h = Planck's constant (6.626068×10^{-34} m^2 kg/s), μB = Bohr Magneton ($9.27400968(31) \times 10^{-24}$ JT^{-1}), g = g-factor (unit-less), v = microwave frequency (GHz; v varied from 9.371051 GHz to 9.3729223 GHz), H = magnetic field (gauss; 3342.52 G).

In most organic free radicals, the electron spin density is delocalized over the entire molecule via the π-bond system. This spin delocalization causes a lack of orbital angular momentum for the unpaired electron so that the EPR signals are very close to the free electron g value, 2.0023. It was observed that time does not have an impact on the free radical species and concentration. No changes in the radical intensity were observed in the EPR after a span of 6 months confirming the stability of free radicals.

Proposed Mechanism for the Grafting of PAA on the GRT Surface

A proposed mechanism for the surface-grafting of GRT particles by PAA is represented in Scheme 1. The stable mechano-free radicals present in the GRT are generated during the grinding of the waste rubber by the turbo-shearing mill grinding process. The process leads to the generation of mechanical forces (under inert conditions) creating mechanochemical effect [22]. Sufficient amount of heat generated during mechanochemical effect can degrade the rubber particles. In order to eliminate the excess heat, pulverization under cryogenic conditions was carried out. These forces are sufficient for rupturing the primary covalent bonds (C—C, C—H, and C—O) and secondary van der Waals or hydrogen bonds thereby creating stable and reactive free radicals on the surface of the GRT particles. These free radicals self-initiate AA polymerization. Stable free radicals were observed by Sato et al. [23] in ground quartz and quartz glass during the grind milling process. Similar process was studied by others on the copolymerization of vinyl acetate initiated by the mechano-free radicals present in PTFE [24, 25].

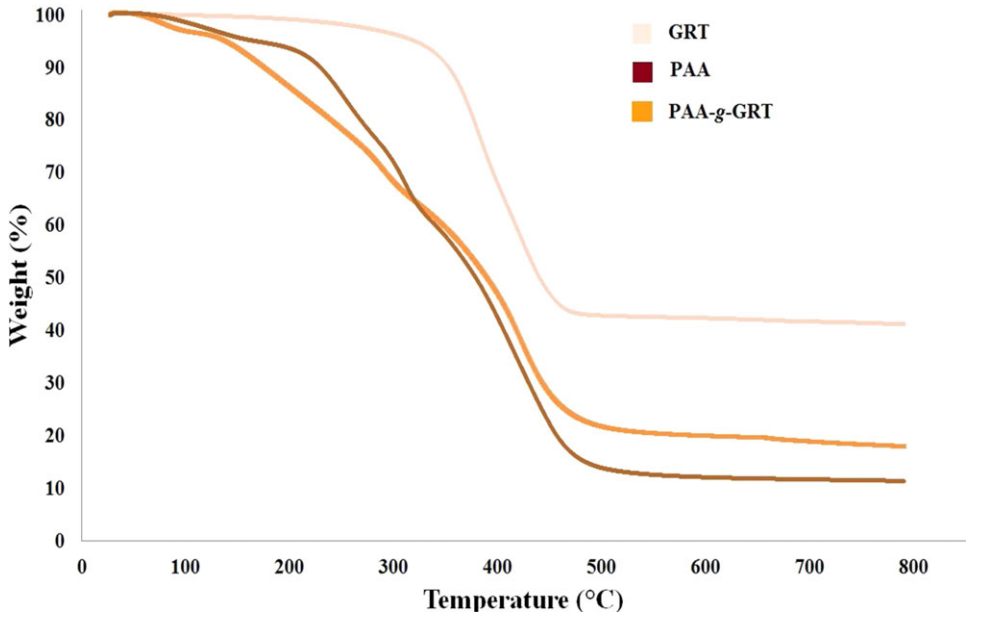

FIG. 4. TGA curves of the neat GRT and PAA-*g*-GRT. [Color figure can be viewed in the online issue, which is available at wileyonlinelibrary.com.]

 DOI 10.1002/pc

Polymerization of AA performed under the same conditions failed to occur in the absence of GRT particles.

ATR-FTIR Analysis of PAA-g-GRT

The structural changes associated with the surface-grafted GRT at different time intervals were analyzed by ATR-FTIR and compared with the neat GRT (Fig. 2). Two peaks were observed at 2846 and 2898 cm^{-1} in the IR spectrum of the neat GRT (Fig. 2a) corresponding to the C—H stretching vibrations. The broad peak observed in the frequency region of 920–1100 cm^{-1} corresponds to the overlap of Si—O—Si asymmetric vibration of SiO_2 and the =C—H bending vibration of GRT [13, 26]. The peaks observed at 1407 and 1446 cm^{-1} is attributed to CH_2 bending and aromatic stretching vibrations of the styrene butadiene/natural rubber (SBR/NR) polymer unit in the GRT and are overlapped with the bending vibrations (1470 and 1385 cm^{-1}) of the CH_3 groups of NR unit [13, 27, 28]. In comparison with the neat GRT, two new peaks (1681 and 3300 cm^{-1}) were observed in the PAA-*g*-GRT and their intensities increase with the increasing time (1, 3, 6, and 12 h, Fig. 2b–e). The above peaks correspond to the carbonyl (C=O) and hydroxyl (O—H) stretching vibrations of PAA. The result suggested that PAA has been successfully grafted onto the GRT surface.

XPS Studies

The PAA-*g*-GRT was further investigated by XPS, an effective surface sensitive technique. Figure 3 shows the C1s spectrum of the neat GRT and PAA-*g*-GRT. The peaks with the binding energies of 288.0 and 288.9 eV in the C1s spectrum of the neat GRT (Fig. 3a) corresponds to the carbonate/C—O and C—O groups produced during the rubber processing. The peak observed at 285.4 eV corresponds to the C—C, C=C, C—H, and CH_2 groups of SBR/NR polymer [13]. The peaks with the binding energies of 286.2, 289.6, and 288.5 eV in the spectrum of PAA-*g*-GRT is attributed to the C—OH, C—O, and O—C=O groups of the PAA attached to the GRT surface (Fig. 3b). In comparison with the neat GRT, the binding energies of PAA-*g*-GRT were slightly shifted. After the self-initiated polymerization, masking of the peak at 285.5 eV and the appearance of new peak at 286.2 eV corresponds to the C—OH group indicated the successful grafting of PAA onto the GRT surface.

Thermogravimetric Analysis

TGA curves of the neat GRT, PAA (polymerized with AIBN initator without any GRT), and PAA-*g*-GRT are shown in Fig. 4. It was found that the PAA-*g*-GRT exhibit a drastic initial weight loss as compared with the neat GRT as well as the PAA. The thermal decomposition temperature at 5% weight loss ($T_{d5\%}$) for the PAA-*g*-GRT was found at 150°C well below the $T_{d5\%}$ for the neat GRT, which registered a higher value at 379°C [29]. The initial weight loss between 70 and 130°C in the PAA-*g*-GRT curve is attributed to the physcially absorbed water [30]. The thermal degradation of neat GRT can be explained by the pyrolytic degradation of the polymer chains (275 to 410°C) followed by the oxidative combus-

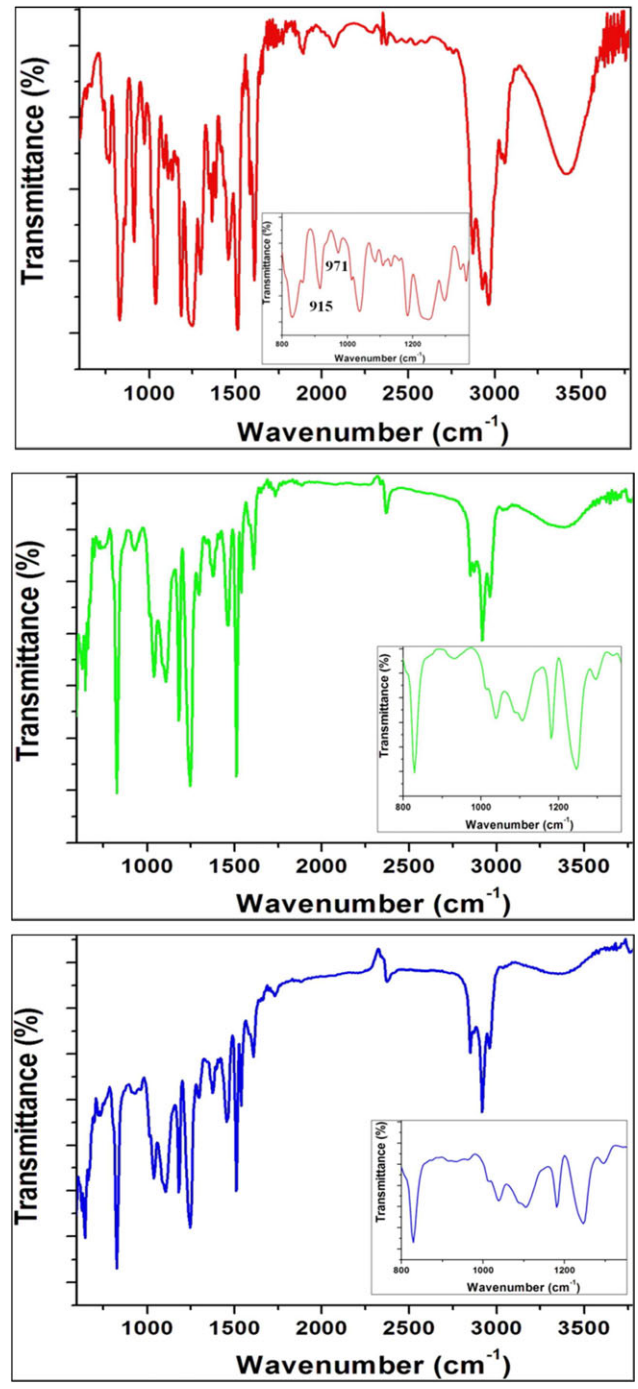

FIG. 5. ATR-FTIR spectra of (a) epoxy resin, (b) cross-linked epoxy, and (c) PAA-*g*-GRT/epoxy composite. [Color figure can be viewed in the online issue, which is available at wileyonlinelibrary.com.]

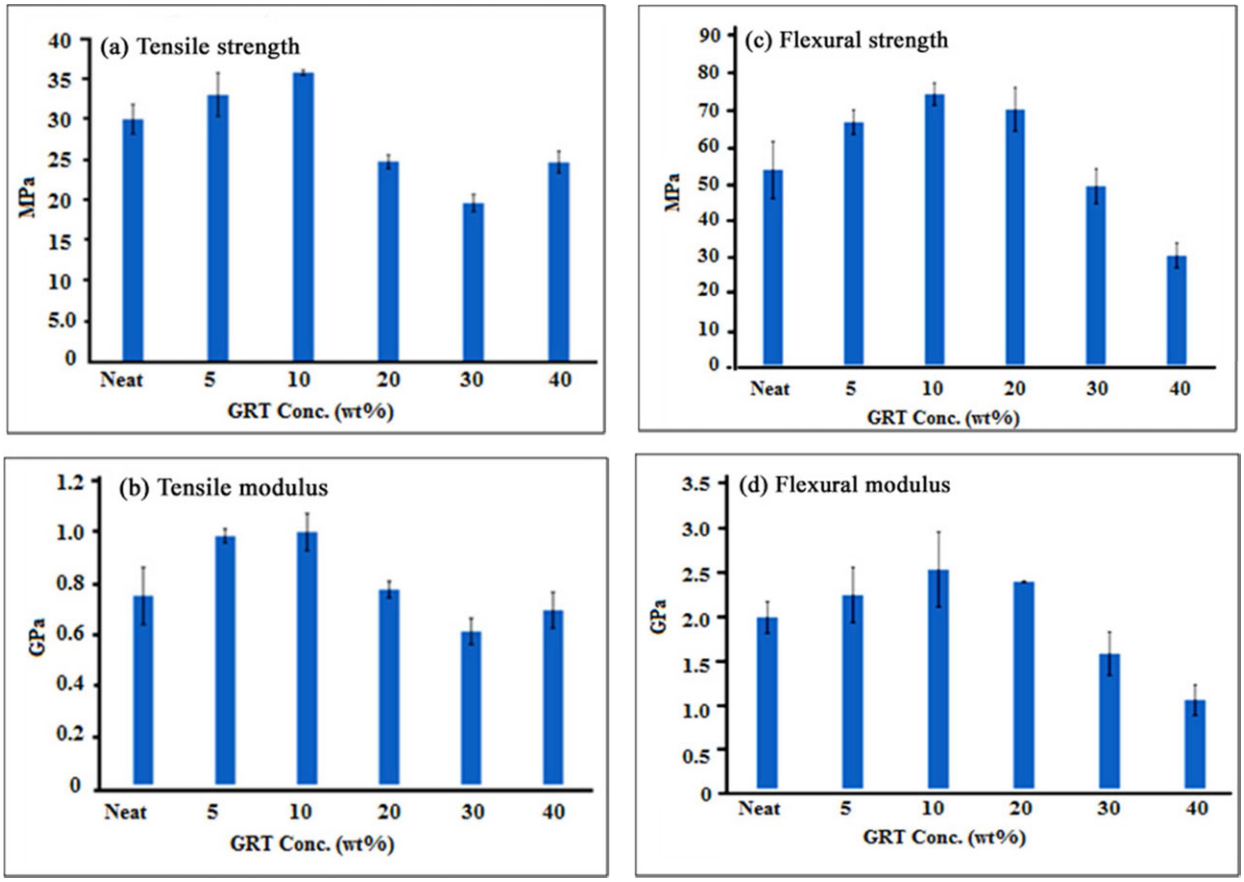

FIG. 6. Mechanical properties of the epoxy and neat GRT/epoxy composites. [Color figure can be viewed in the online issue, which is available at wileyonlinelibrary.com.]

tion of carbon black (450–650°C) and pyrolyzed char in the presence of air (650–800°C).

ATR-FTIR Analysis

Figure 5 shows the FTIR spectra of epoxy resin, cured or cross-linked epoxy, and PAA-*g*-GRT/epoxy composite. The IR spectrum of epoxy resin showed the presence of characteristic absorption bands at 3030 and 3056 cm^{-1} correspond to the aromatic C—H and CH—OH stretching vibrations. The absorption bands at 2964, 2929, and 2872 cm^{-1} attributed to the $—CH_2$ and $—CH_3$ asymmetrical and symmetrical stretching vibrations. The band at 1036 cm^{-1} corresponds to the Ar—O—C stretching vibration. The epoxy groups in IR spectrum was proved by the presence of breathing vibration modes at 971 (bending C—H epoxy) and 915 cm^{-1} (C—O epoxy). The peak at 830 cm^{-1} is ascribed to the aromatic 1,4 substitution of epoxy resin [31]. The absence of the oxirane ($\nu_{\overset{O}{\diagup\diagdown}C-C}$) peaks at 971 and 915 cm^{-1} and the absence of these peaks in the cured epoxy and PAA-*g*-GRT/epoxy composite confirmed that the curing process occurred based on the addition reaction between epoxy and amine. Most of the peaks of GRT and PAA were overlapped with the epoxy peaks.

Mechanical Properties

Figure 6 shows the tensile and flexural properties of the cured epoxy and neat GRT/epoxy composites (made according to the ASTM D 638 and D 790) with different weight fractions of the GRT. The tensile strength of cured epoxy was 30.24 MPa, which was lower than 5 and 10% neat GRT/epoxy composites, but higher than those of the composites with 20, 30, and 40% GRT (Fig. 6a). The initial 120% increase in the tensile strength of composite with 10% GRT is indicative of good adhesion between the GRT particles and the epoxy matrix, resulting in a positive toughening effect between the two. Generally, fillers are added to the polymer matrix to produce a material with low flexiblity having higher tensile strength and modulus. This may be attributed to the reduced molecular mobility of the polymer chains [32, 33]. The decrease in strength at higher GRT content may be due to the disruption of the epoxy matrix as more GRT particle are added. When compared with the composite with 30% GRT, a slight increase in the tensile strength was observed for 40% composite. This may be due to the inhomogenity of GRT particles in the epoxy matrix. The mechanical properties of the composite containing filler dispersed in the polymer matrix depends on the structural continuity and interfacial adhesion between the filler and matrix [10].

 DOI 10.1002/pc

The decrease in the tensile strength at higher GRT concentration was due to the nonadherence of the GRT particles with the epoxy matrix and the random distribution of the excess GRT particles in the epoxy network. The nonadherence of the GRT particles create voids in the epoxy matrix and lead to agglomeration. This may result in discontinuity of the structure and generates stress around the GRT particles reducing the load capability resulitng in the decrease of overall strength of the composite. The variation of tensile modulus of the cured epoxy and neat GRT/epoxy composites is shown in Fig. 6b. The tensile modulus of cured epoxy was 0.71 GPa and that of 10% neat GRT/epoxy composite was 1.08 GPa; it dropped to 0.62 GPa when the concentation of GRT is 30%. An increase of 130% modulus was observed for composite with 10 wt% GRT. The modulus of composite falls to a lower value at higher GRT concentration. This may be attributed to the decrease in brittleness of the epoxy matrix as more GRT particles were added to the epoxy.

Figure 6c shows the flexural strength of cured epoxy and neat GRT/epoxy composites. The flexural strength of cured epoxy was 53.89 MPa and increased to 74.51 MPa when the GRT content in composite was 10% but the strength gradually decreases from 74.51 to 30.56 MPa as the concentration of GRT increases from 10 to 40% in the composite. Similar trend was observed for the flexural modulus as well. The highest modulus of 2.53 GPa was obtained for the composite with 10% GRT. The increase in flexural strength (138%) and modulus (127%) was observed for the composite with 10% GRT as compared with the cured epoxy. It has been shown that a better dispersion of the filler in the epoxy matrix increases the flexural modulus of the composite materials [11], which was further explained by the percolation theory [12]. According to the theory, there is an associated zone corresponding to the each particle in the polymer matrix which is affected by a stress. The matrix zones join together when the distance between the particle is smaller enough resulting in the formation of a percolation effect. This effect of interfacial properties between the GRT particles and epoxy matrix plays an important role in stress transfer and the elastic deformation of the matrix to the GRT particles. For a constant GRT loading, there is an increase in the contact area of the matrix, which increases the interfacial stiffness and facilitates the effective stress transfer, thereby resulting in the increase of modulus. At higher GRT content, the composite modulus decreases due to the particle agglomeration.

Figure 7 shows the tensile and flexural properties of the PAA-*g*-GRT/epoxy composites. The tensile strength of PAA-*g*-GRT/epoxy composites decreases as the PAA-*g*-GRT content increases in the composite indicating a

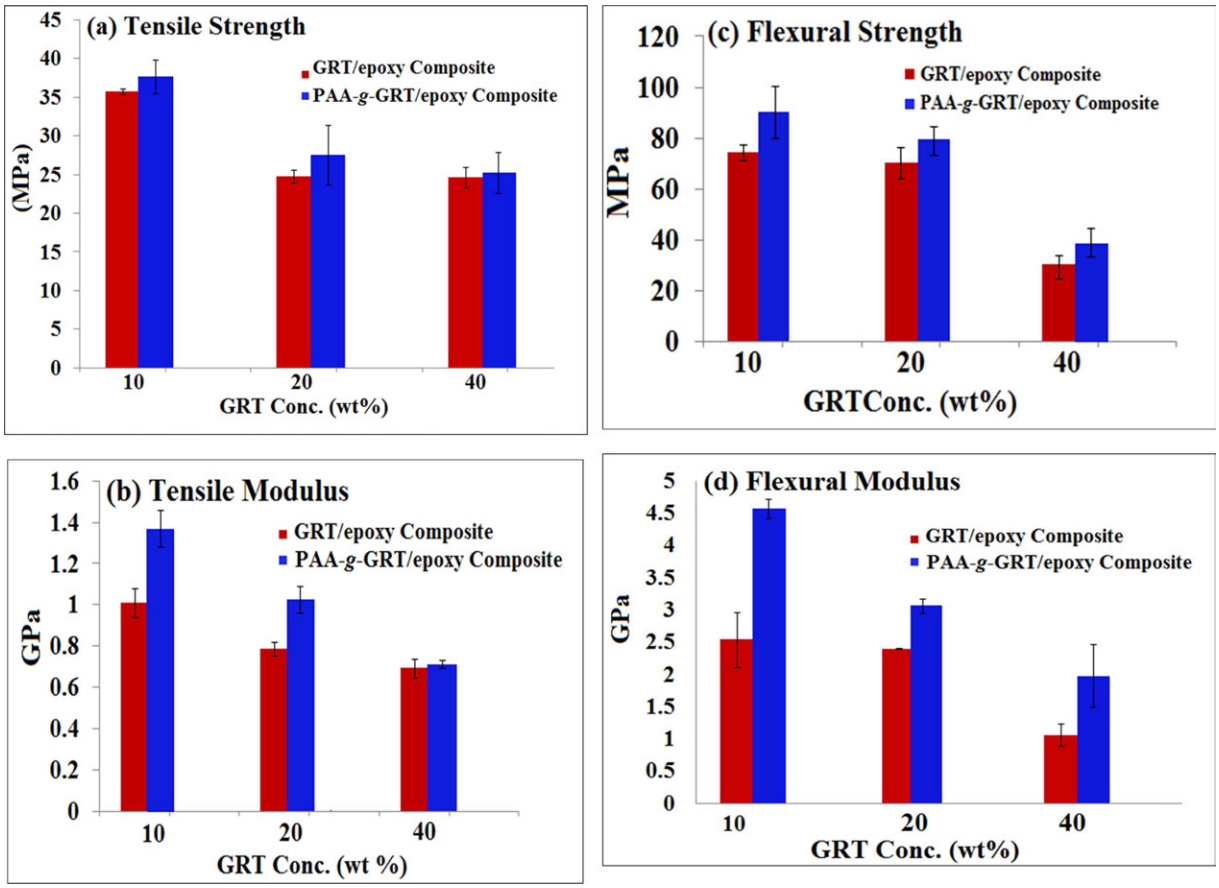

FIG. 7. Mechanical properties of the GRT and PAA-*g*-GRT/epoxy composites. [Color figure can be viewed in the online issue, which is available at wileyonlinelibrary.com.]

TABLE 1.

Composite Samples	Elongation at break%
Neat Epoxy Composite	56
Epoxy/ GRT (10 wt %)	41
Epoxy/ GRT (20 wt %)	48
Epoxy/ GRT (40 wt %)	51
Epoxy/ PAA-g-GRT (10 wt %)	21
Epoxy/ PAA-g-GRT (20 wt %)	42
Epoxy/PAA-g- GRT (40 wt %)	45

decrease in the toughness (Fig. 7a). When compared with the neat GRT/epoxy composites, an increase in the tensile modulus (Fig. 7b) and flexural strength (Fig. 7c), as well as a significant increase in the flexural modulus (Fig. 7d) was observed for the PAA-*g*-GRT/epoxy composites. A remarkable increase in tensile and flexural modulus of 180% was observed for the composite with 10% PAA-*g*-GRT, whereas 186% increase was calculated for the 40% composite. In comparison with the cured epoxy, 10% PAA-*g*-GRT/epoxy composite registered a 229% increase in the modulus indicating an increase in the stiffness of the composite. Therefore, 10% GRT is the optimal to achieve improved property of the composite.

Elongation at break % with respect to the different wt% of GRT is shown in Table 1. The neat epoxy composites exhibit a higher elongation at break % in comparison to GRT/epoxy composites and PAA-*g*-GRT/epoxy composites with different wt% of GRT and PAA-*g*-GRT, respectively. GRT/epoxy and PAA-*g*-GRT composites with 10 wt% GRT, showed a lower elongation at break % with higher tensile strength and modulus. This may be attributed

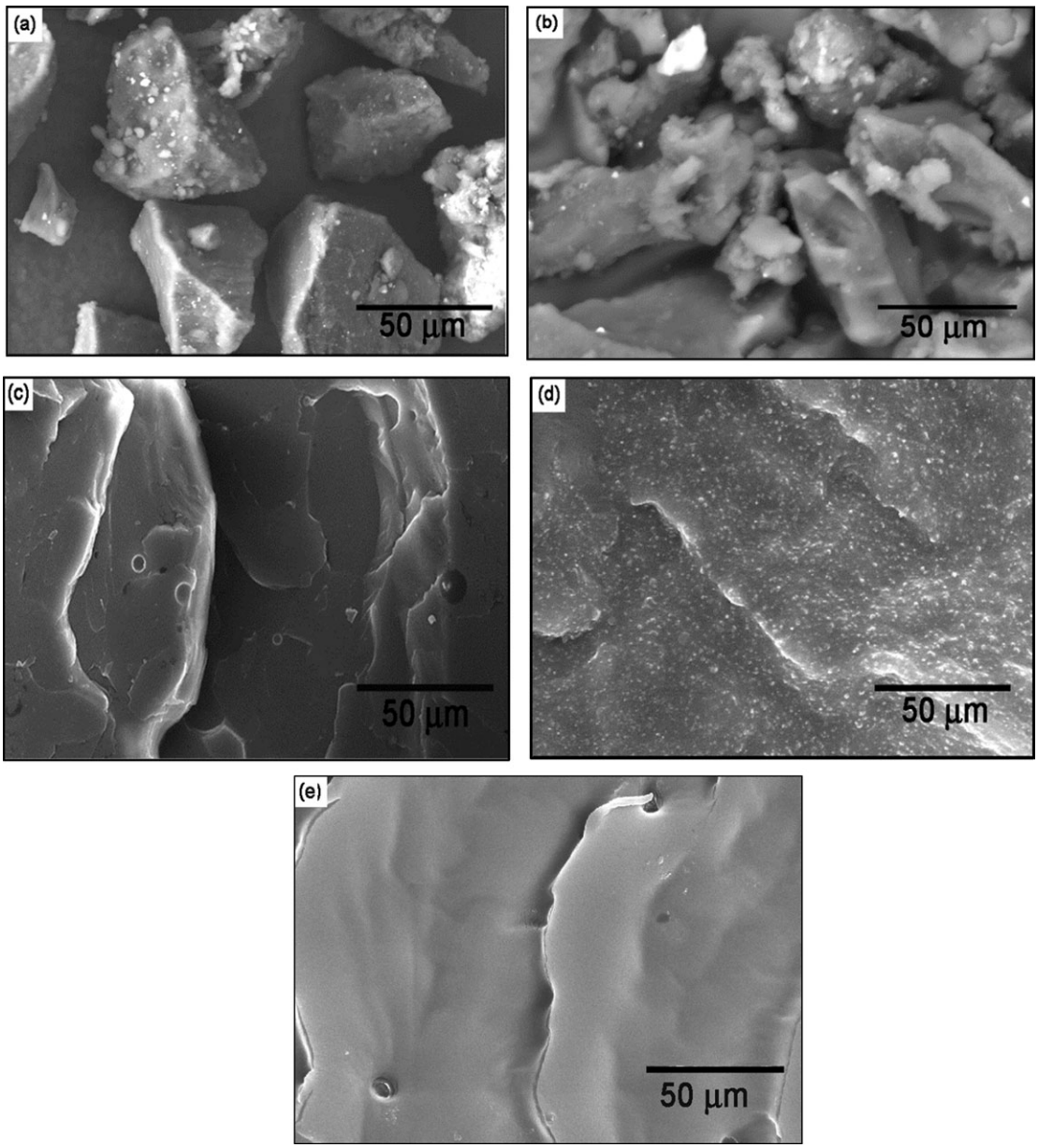

FIG. 8. SEM images of (a) neat GRT, (b) PAA-*g*-GRT, (c) neat epoxy, (d) PAA-*g*-GRT (40%)/epoxy, and (e) neat GRT (40%)/epoxy composites.

 DOI 10.1002/pc

to the fact that it takes more force to elongate a material having high strength and modulus. Similar trend was observed in the case of PAA-g-GRT/epoxy composites.

Morphology

Figure 8 shows the SEM images of neat GRT, PAA-*g*-GRT, epoxy, PAA-*g*-GRT (40%)/epoxy, and GRT (40%)/epoxy composites. From Fig. 8a, one can see that the as-received GRT particles showed a typical morphology with surface roughness. The GRT particles were in micron range, which is consistent with the supplier's statement. The apparent physical nature of GRT particles (Fig. 8b) changed after surface-grafting by PAA and the surface roughness decreases. The morphology of PAA-*g*-GRT changed remarkably after the formation of composite with epoxy (Fig. 8d). This is due to the reduction in the hardness of the composite material, which is supported by our elongation at break results. As a comparison, the SEM images of neat epoxy and neat GRT/epoxy is given (Fig. 8c and e).

CONCLUSIONS

The self-initiated free radical polymerization of AA on the surface of economically viable mechanochemically devulcanized GRT particles were successfully achieved via the stable mechano-free radicals present in the GRT. The EPR analysis confirmed the presence of stable free radicals present in the GRT with a *g*-factor of 2.0035, which is similar to the *g*-factor of free electrons. The PAA-*g*-GRT/epoxy composites showed significant enhancement in the mechanical properties. In comparison with the neat GRT/epoxy composite, an increase in the tensile and flexural modulus of 180% was observed in the PAA-*g*-GRT/epoxy composite. The PAA grafted GRT resulted in a better filler material, which could adhere well to the epoxy matrix. The GRT could be a cost effective and environmentally safe approach to replace the conventional free radicals and costly fillers.

ACKNOWLEDGMENTS

The authors would like to extend thanks to the Lehigh Technologies, LLC for their supply of raw materials. We would like to acknowledge the Department of chemistry, Clemson university and Robert A. Welch Foundation (Grant No. AT-0041) at the University of Texas at Dallas for their financial support.

REFERENCES

1. D.Y. Wu, S. Bateman, and M. Partlett, *Compos. Sci. Technol.*, **67**, 190 (2007).
2. R.H. Snyder, *Scrap tires: Disposal and reuse*, Society of Automotive Engineers International, Warrendale, PA. (1998).
3. Rubber manufacturing Association (RMA). Scrap tire market in the United States (2007).
4. S.K. De, *Prog. Rubber. Plast. Technol.*, **17**, 113 (2001).
5. W. Klingensmith and K.C. Baranwal, *Rubber World.*, **218**, 41 (1998).
6. S.B. Liang and Y.C. Hao, *Adv. Powder Technol.*, **11**, 187 (2000).
7. D. Mangaraj, *Rubber Chem. Technol.*, **78**, 536 (2005).
8. W. Dierkes, *Rubber India.*, **48**, 9 (1996).
9. Y.W. Song, H.S. Do, H.S. Joo, D.H. Lim, S. Kim, and H.J. Kim, *J. Adhesion Sci. Technol.*, **20**, 1357 (2006).
10. A.A. Yehia, M.A. Mull, M.N. Ismail, Y.A. Hefny, and E.M. Abdel-Bary, *J. Appl. Polym. Sci.*, **93**, 30 (2004).
11. X. Zhang, X. Zhu, M. Liang, and C. Lu, *J. Appl. Polym. Sci.*, **114**, 1118 (2009).
12. A.M. Shanmugharaj, J.K. Kim, and S.H. Ryu, *Polym. Test.* **24**, 739 (2005).
13. A.K. Naskar, S.K. De, and A.K. Bhowmick, *Rubber Chem. Technol.*, **74**, 645 (2001).
14. A.K. Naskar, A.K. Bhowmick, and S.K. De, *J. Appl. Polym. Sci.*, **84**, 622 (2002).
15. M. Pittolo and R.P. Burford, *J. Mater. Sci.*, **21**, 1769 (1986).
16. I. Fuhrmann and J. Karger-Kocsis, *J. Appl. Polym. Sci.*, **89**, 1622–1628, (2003).
17. S. Coiai, E. Passaglia, F. Ciardelli, D. Tirelli, F. Peruzzotti, and E. Resmini, *Macromol. Symp.*, **234**, 193 (2006).
18. S. Coiai, E. Passaglia, and F. Ciardelli, *Macromol. Chem. Phys.*, **207**, 2289 (2006).
19. K.P.U. Perera, D.W. Smith, J.C. Moreland, and K. Wallace, U. S. Patent **0**,060, 711 A1 (2007).
20. M. Banda, A.K. Naskar, P.U. Perera, C. Moreland, T. Hodge, K. Wallace, H.W. Beckham, and D.W. Smith, *Rubber Chem. Technol.*, **85**, 68 (2012).
21. Y.A. Aggour, A.S. Al-Shihri, and M.R. Bazzt, *Open J. Polym. Chem.*, **2**, 70 (2012).
22. F. Cataldo, F. Padella, and F. Cavalieri, *J. Appl. Polym. Sci.*, **90**, 1631 (2003).
23. M. Sato, T. Ogata, and M. Hasegawa, *Powder Technol.*, **85**, 269 (1995).
24. J. Sohma and M. Sakaguchi, *J. Appl. Polym. Sci.*, **22**, 2915 (1978).
25. J. Sohma, M. Sakaguchi, and N. Kurokawa, *J. Appl. Polym. Sci.*, **25**, 1209 (1980).
26. B. McCool, L. Murphy, and C.P. Tripp, *J. Colloid Interface Sci.*, **296**, 294 (2006).
27. S. Gunasekharan, R.K. Natarajan, and A. Kala, *Spectrochim. Acta Part A.*, **68**, 323 (2007).
28. S. Roy and P.P. De, *Polym. Test.*, **11**, 3 (1992).
29. S.H. Lee, M. Balasubramanian, and J.K. Kim, *J. Appl. Polym. Sci.*, **106**, 3209 (2007).
30. S. Dubinsky, G.S. Grader, G.E. Shter, and M.S. Silvertein, *Polym. Degrad. Stab.*, **86**, 171 (2004).
31. G. Nikolic, S. Zlatkovic, M. Cakic, S. Cakic, C. Lacnjevac, and Z. Rajic, *Sensors.*, **10**, 684 (2010).
32. A.J. Gu, S.W. Kuo, and F.C. Chang, *J. Appl. Polym. Sci.*, **79**, 1902 (2001).
33. Y. Yang, Z.K. Zhu, J. Yin, X.Y. Wang, and Z.N Qi, *Polymer.*, **40**, 4407 (1999).